

Ab Initio Studies of Properties of Small Potassium Clusters

Arup Banerjee,[†] Tapan K. Ghanty,^{*,‡} and Aparna Chakrabarti[§]

Laser Physics Application Division, Raja Ramanna Centre for Advanced Technology, Indore 452013, India, Theoretical Chemistry Section, Chemistry Group, Bhabha Atomic Research Centre, Mumbai 400 085, India, and Semiconductor Laser Section, Raja Ramanna Centre for Advanced Technology, Indore 452013, India

Received: August 25, 2008; Revised Manuscript Received: October 3, 2008

We have studied the properties of various isomers of potassium clusters containing even number of atoms ranging from 2 to 20 at the ab initio level. The geometry optimization calculations of the isomers of each cluster are performed by using all-electron density functional theory with gradient corrected exchange-correlation functional. Using the optimized geometries of different isomers we investigate the evolution of binding energy, ionization potential, and static polarizability with the increasing size of the clusters. The polarizabilities are calculated by employing Möller-Plesset perturbation theory and time-dependent density functional theory. The polarizabilities of dimer and tetramer are also calculated by employing large basis set coupled cluster theory with single and double excitations and perturbative triple excitations. The time-dependent density functional theory calculations of polarizabilities are carried out with two different exchange-correlation potentials: (i) an asymptotically correct model potential and (ii) within the local density approximation. A systematic comparison with the other available theoretical and experimental data for various properties of small potassium clusters mentioned above has been performed. These comparisons reveal that both the binding energy and the ionization potential obtained with gradient-corrected potential match quite well with the already published data. Similarly, the polarizabilities obtained with Möller-Plesset perturbation theory and with model potential are quite close to each other and also close to experimental data.

I. Introduction

During last two decades rapid progress in the experimental methods of producing atomic and molecular clusters in controlled fashion along with the development of sophisticated theoretical tools to handle such finite fermionic systems at the ab initio level led to emergence of the field of cluster science as one of the most exciting and productive disciplines of physics, chemistry, and material science. Metal clusters, especially those of alkali-metal atoms Li, Na, and K, played an important role in the development of cluster physics as a branch of modern physics and chemistry. Interest in the study of alkali-metal clusters grew with the pioneering work of Knight and co-workers.¹ These researchers discovered that certain clusters, those with magic numbers 8, 20, 34, 40,... of atoms, are more stable and consequently were found more abundantly in the mass spectra of these clusters. The existence of magic number clusters is attributed to the electronic shell structure of the clusters. Other properties like ionization potential, electron affinity, and static polarizabilities of metal clusters also show significance of the shell structure. Besides these, photoabsorption cross sections have also been measured for alkali metal clusters and have been investigated theoretically at various levels. A large body of theoretical work on the electronic structure and optical response properties of alkali-metal clusters exists in the literature. The majority of the theoretical work has been carried out by employing density functional theory (DFT) and time-dependent

DFT (TDDFT) within the spherical jellium background model (SJBM) (see the review articles in refs 2 and 3). The SJBM replaces the discrete ionic structure of clusters by a spherically symmetric uniform positive charge background thus making it possible to carry out calculations for the optical response properties of reasonably large clusters of around 100 atoms.^{2,4} In last ten years or so, several all-electron ab initio calculations devoted to the ground state and the optical response properties of sodium clusters taking into account the actual geometrical arrangement of the sodium atoms have been reported in the literature.^{5–17} However, these calculations could handle clusters with sizes smaller than those that could be studied by performing jellium-based calculations. We should mention here that the calculations of structure, electronic, and static polarizability of small sodium and lithium clusters have also been performed by employing ab initio correlated wave function based methods like MP2, MP4, and SCF-CI.^{13,18,19}

We note here that among these numerous studies involving properties of alkali-metal clusters only very few are devoted to the calculations of properties of potassium atom clusters. This is quite surprising considering the fact that the experimental results for the ionization potential, static polarizability, and photoabsorption spectra of potassium clusters as functions of cluster size were reported very early in the development of cluster physics.^{1,20} Along with the calculations of sodium clusters few SJBM based studies within the realm of DFT and TDDFT pertaining to the evolution of binding energies, ionization potentials, and static polarizabilities of potassium clusters exist in the literature.^{21–28} Likewise, a few studies of the potassium clusters at the ab initio level taking into account the detailed ionic structure employing various approaches like configuration interaction (CI),^{29,30} many-body perturbation theory,³¹ DFT coupled with pseudopotential,³² and coupled cluster theory³³

* Address correspondence to this author. E-mail: tapang@barc.gov.in.

[†] Laser Physics Application Division, Raja Ramanna Centre for Advanced Technology.

[‡] Theoretical Chemistry Section, Chemistry Group, Bhabha Atomic Research Centre.

[§] Semiconductor Laser Section, Raja Ramanna Centre for Advanced Technology.

have also been reported in the literature. However, these studies were restricted to very small sized clusters containing a maximum of up to seven potassium atoms³¹ and investigated ground-state properties like bond lengths, binding energies, and ionization potentials. To the best of our knowledge only one ab initio level calculation of static polarizability of up to 10 atom cluster by DFT/TDDFT methods appeared very recently in the literature.³⁴ In the present paper our main aim is to investigate systematically the size evolution of various ground state properties like the binding energy (BE), ionization potential (IP), and response property like static polarizability at the ab initio level for potassium clusters with an even number of atoms ranging from 2 to 20 atoms. To this end we employ the ab initio DFT-based method with gradient corrected exchange-correlation (XC) potential for geometry optimization and three methods for the calculations of polarizabilities, namely, the second-order Möller–Plesset perturbation theory (MP2),³⁵ coupled cluster theory with single and double excitations and perturbative triple excitations (CCSD(T)),³⁶ and TDDFT with asymptotically correct XC potential. The high computational cost and time involved in CCSD(T) and MP2 based calculations restrict the maximum size of the cluster that could be handled by this approach. In this paper we perform MP2-based polarizability calculations for clusters containing a maximum of up to 14 atoms and CCSD(T)-based calculations are performed for dimer and tetramer only. Nonetheless these results provide a way to check the correctness and consistencies of the results obtained by us by employing various methods. At the outset we mention that in all our calculations of the polarizability, the effect of vibrations has been ignored. So the results presented in this paper include only the electronic part of the static polarizability tensor.

We note that to carry out ab initio calculations of the ground state properties mentioned above and the polarizabilities of clusters which go beyond the jellium model, it is necessary to have the knowledge of the ionic structure of the clusters. However, apart from the dimer (K_2), experimental results for the cluster structures are not available. For small clusters ranging from K_3 to K_7 some theoretical results are available in the literature and we make use of these structures for our work. Unfortunately, beyond K_8 even theoretical results are scarce in the literature. We note here that with the increase in size, a cluster can exist in several possible configurations (isomers). In this paper we do not attempt to determine the global minimum geometries of the potassium clusters. We rather assume that the optimal configurations of potassium clusters should possess the symmetry elements of the corresponding sodium clusters. This assumption is consistent with the results of ref 37 in which it has been shown that global minima structures of sodium and potassium clusters obtained by employing the genetic algorithm and basin hopping Monte Carlo method with a model many-body potential are identical (except for the cluster containing 16 atoms) for clusters containing up to 20 atoms. In this paper to obtain the geometry of each potassium cluster beyond K_4 , we use structures with the same symmetry elements as those of sodium clusters reported in refs 11 and 12. We employ the DFT-based geometry optimization scheme with the Becke-Perdew (BP86)³⁸ exchange-correlation (XC) potential within the generalized gradient approximation (GGA) as this potential is known to yield reliable geometries.³⁹ These optimized structures of potassium clusters are then employed to carry out calculations of ionization potentials and polarizabilities.

The calculation of response property like polarizabilities by the TDDFT approach requires approximating the forms of XC functionals. It is well-known that the accuracy of the results

for response properties obtained via TDDFT crucially depends on the nature of the XC potential, especially its behavior in the asymptotic region.^{40,41} Keeping this in mind, we carry out all-electron TDDFT-based calculations of static polarizabilities of potassium clusters with a model XC potential, called statistical average of orbital potentials (SAOP), which has desirable properties both in the asymptotic and in the inner regions of a molecule.^{42,43} The choice of SAOP is also motivated by the results of refs 10 and 17, where it has been shown that SAOP polarizability and excitation energies of sodium clusters agree well with the experimental data. Furthermore, to study the effect of XC potential on the polarizabilities, calculations of polarizabilities are also carried out with less accurate XC potential under local density approximation (LDA). It is well-known that the static polarizabilities of sodium clusters obtained by employing DFT and TDDFT within SJBm are generally underestimated in comparison to the corresponding ab initio and experimental results. However, such a comparison of the SJBm, ab initio, and experimental results does not exist for potassium clusters. To test the accuracy of the jellium model, we compare the results for the static polarizability of 8 and 20 atom clusters (as jellium-based results are available in the literature) obtained by employing LDA XC potential in the realm of SJBm with corresponding ab initio and experimental data. The rest of the paper is organized as follows: In Section II we discuss the theoretical methods employed to calculate the optimized geometry, BE, IP, and static polarizabilities of potassium clusters. Results of our calculations are presented in Section III, and the paper is concluded in Section IV.

II. Theoretical Methods

In this work we study different properties of small sized potassium clusters on the basis of all-electron ab initio methods. For this purpose we use ADF program package⁴⁴ for DFT- and TDDFT-based calculations and GAMESS electronic structure code for carrying out post-Hartree–Fock MP2 and CCSD(T) calculations.⁴⁵ We optimize geometries of various isomers of the clusters containing an even number of atoms ranging from 2 to 20 atoms. The geometry optimizations of all the clusters have been performed through DFT-based calculations by employing a triple- ξ Slater-type orbital (STO) basis set with two added polarization functions (TZ2P basis set of the ADF basis set library) along with the Becke-Perdew (BP86) XC potential.³⁸ The geometry optimization involves finding local minima on the multidimensional potential energy surface. The starting geometry of the cluster plays an important role in the optimization procedure. In the present calculations for each cluster beyond K_4 we have considered more than one starting geometry, which are compiled from already available optimized structures of sodium clusters.^{11,12} Our aim in this paper is to study how the properties of potassium clusters vary with different structures and also sizes. We make no assumption regarding the core electrons and perform all-electron geometry optimization calculations. All the optimizations are carried out with the convergence criteria for the norm of energy gradient and energy, fixed at 10^{-4} atomic units (au) and 10^{-6} au, respectively.

In this paper we further calculate the static polarizabilities of potassium clusters by employing MP2-, CCSD(T)-, and TDDFT-based methods. The calculations of polarizabilities with MP2 and CCSD(T) have been carried out by employing the finite field approach available in the GAMESS electronic structure code. The finite field approach makes use of the perturbative series expansion of the energy E in terms of the components of a static uniform electric field F given by,

$$E(\vec{F}) = E(0) + \sum_i \mu_i F_i + \frac{1}{2} \sum_{ij} \alpha_{ij} F_i F_j + \dots \quad (1)$$

where $E(0)$ is the energy of the system in the absence of the applied electric field, $\vec{\mu}$ is dipole moment, and α_{ij} ($i, j = x, y, z$) is the dipole polarizability tensor. The components of the polarizability tensor are obtained as the second-order derivatives of the energy with respect to the components of the electric field,

$$\alpha_{ij} = \left(\frac{d^2 E}{dF_i dF_j} \right)_{F=0} \quad (2)$$

The derivatives are calculated numerically by applying fields of 0, 0.001, and 0.002 au along $\pm x$, $\pm y$, and $\pm z$ directions and mean polarizability is calculated from the diagonal elements of polarizability tensor as

$$\bar{\alpha} = \frac{1}{3} (\alpha_{xx} + \alpha_{yy} + \alpha_{zz}) \quad (3)$$

All MP2 and CCSD(T) calculations have been performed with valence triple- ζ polarized Gaussian basis sets of Sadlej and Urban⁴⁶ for potassium atom.

On the other hand, TDDFT calculation of polarizability is based on the linear response theory of many-body systems and employs exact analytical expressions for polarizability in terms of the moment of the first-order induced density. To avoid digression we refer the readers to ref 47 for detailed description of the linear response theory based method which is adopted in the ADF program package for obtaining polarizability. We note here that TDDFT-based method gives frequency dependent polarizability but here we focus our attention on the static or zero-frequency polarizability. We also mention here that unlike the finite field approach the calculation of polarizability based on linear response theory of many-body system does not require any explicit specification of the magnitude of the applied field. It has already been mentioned that TDDFT-based response property calculation requires approximating the XC functional at two different levels. The first one is the static XC potential needed to calculate the ground-state Kohn–Sham (KS) orbitals and orbital energies. The second approximation is needed to represent the XC kernel $f_{XC}(r, r', \omega)$ which determines the XC contribution to the screening of an applied field. For the XC kernel, we use reasonably accurate adiabatic local density approximation (ALDA).⁴⁸ On the other hand, for the static XC potential needed to calculate the ground state orbitals and energies, two different choices have been made. These are (i) the standard potential under local density approximation (LDA) as parametrized by Vosko, Wilk, and Nussair⁴⁹ and (ii) the model potential SAOP possessing correct behavior for both inner and asymptotic regions.^{42,43} The results obtained by these two XC potentials are compared in order to investigate the effect of XC potential on the results for the polarizability. The calculations of polarizabilities of potassium clusters by TDDFT-based method are carried out by using large Slater type orbital (STO) basis sets. It is well-known that for accurate calculations of response properties it is necessary to have large basis sets with both polarization and diffuse functions. For our purpose, we have chosen one of the largest all-electron even-tempered basis sets ET-QZ3P-2DIFFUSE with two sets of diffuse functions consisting of (13s,10p,5d,3f) functions for K available in the ADF basis set library. The application of basis set with diffuse functions often leads to the problem of linear dependencies. Such problems have been circumvented by removing linear combinations of functions corresponding to small eigenvalues of the

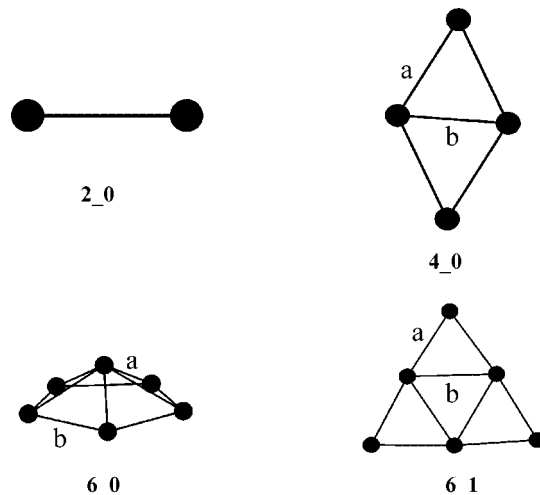


Figure 1. Optimized ground-state geometries of K_2 , K_4 , and K_6 clusters. Letters denote the dimensions tabulated in Table 1.

overlap matrix. We expect that the size of the chosen basis set will make our results very close to the basis-set limit. We note here that the present study involves only even clusters: the reason being that the linear response theory has not been implemented in ADF package for odd clusters. However, though finite field calculations are possible to carry out for odd clusters in ADF it is not implemented with SAOP. Since our one aim is to calculate response properties using SAOP and assess the goodness of this XC potential, we leave out the odd clusters in the present study.

III. Results and Discussion

We begin this section with the discussion on the results of our geometry optimization calculations followed by the results for BE, IP, and polarizabilities of clusters consisting of an even number of atoms ranging from 2 to 20. We compare the results of our calculations with the available experimental data and also results of other theoretical works performed both within the framework of the jellium model and beyond, using DFT or correlated wave function-based methods, and assess the level of accuracy of different theoretical approaches.

A. Ground State Properties of K_n clusters. The optimized structures of potassium clusters, considered in the present study, with an even number of atoms up to 20 are shown in Figure 1 ($n = 2, 4$, and 6) and Figure 2 ($n \geq 8$). The indices n and m in the label n_m assigned to each cluster in these figures denote the number of atoms and the rank in the increasing energy order. To perform the geometry optimization calculations of potassium clusters, we consider for each cluster different configurations with the same symmetry elements as reported for sodium clusters in refs 11 and 12. Then we optimize each configuration using the DFT geometry optimization procedure as is implemented in the ADF package of programs.⁴⁴ Now we present the results for the BE per atom and the average interatomic distances for all the isomers for each cluster. We tabulate the results in two parts. In Table 1, we present the results for K_2 , K_4 , and K_6 clusters and compare them with the other theoretical^{29–32,34} and experimental (for dimer)⁵⁰ data available in the literature. On the other hand, the results for the K_8 and higher clusters are presented in Table 2. Beyond K_{10} no data are available for comparison. We calculate BE, which is presented in Tables 1 and 2 by employing the formula

$$E_b(K_n) = nE(K) - E(K_n) \quad (4)$$

where $E(K_n)$ and $E(K)$ are the total energies of a neutral n -atom potassium cluster K_n and an isolated single potassium atom,

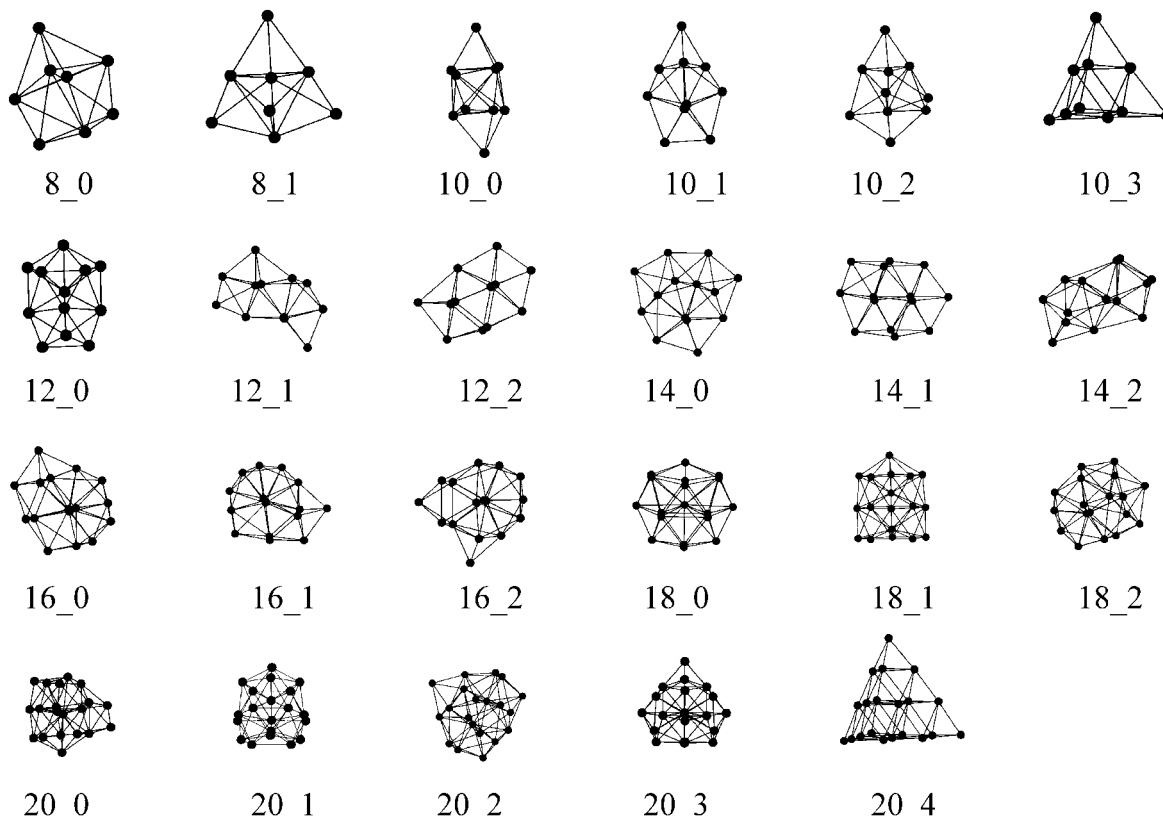


Figure 2. Optimized geometries of potassium clusters K_n with $n = 8-20$. Binding energy per atom and average interatomic distance for these clusters are tabulated in Table 2.

TABLE 1: Comparison of Binding Energy Per Atom (in eV), Bond Length, and Average Interatomic Distance $\langle R \rangle$ (in angstroms) for K_2 , K_4 , and K_6 Clusters

$K_{n,m}$	ref	$-BE/n$	bond length	$\langle R \rangle$
$K_{2,0}$	present	0.25	3.93	3.94
	ref 31	0.19	4.22	4.22
	ref 29	0.21	4.21	4.21
	ref 30	0.32	3.84	3.84
	ref 32	0.26	4.05	4.05
	ref 33	0.27	3.92	3.92
	ref 50 (exptl)	0.25	3.90	3.90
$K_{4,0}$	present	0.31	$a = 4.44, b = 3.98$	4.34
	ref 29	0.19	$a = b = 4.90$	4.90
	ref 30	0.37	$a = b = 4.44$	4.44
	ref 31	0.28	$a = b = 4.78$	4.78
	ref 32	0.34	$a = 4.42, b = 3.92$	4.44
	ref 34		$a = 4.49, b = 4.02$	4.40
$K_{6,0}$	present	0.39	$a = 4.47, b = 4.31$	4.34
	ref 30	0.44	$a = b = 4.50$	4.50
	ref 31	0.37	$a = b = 4.65$	4.65
	ref 34		$a = 4.35, b = 4.57$	4.46
$K_{6,1}$	present	0.39	$a = 4.29, b = 4.60$	4.39
	ref 30	0.42	$a = b = 4.28$	4.28
	ref 31	0.36	$a = b = 4.65$	4.65

respectively. Note that according to eq 4, BE is a negative number for a bound structure and a larger value implies a more stable structure. The second quantity for which results are presented in Tables 1 and 2 is the average interatomic distance in each isomer of a cluster. This quantity is computed by employing the corresponding optimized structure and considering only interatomic distances smaller than 5.076 Å, which is 10% higher than the nearest neighbor distance in the bcc lattice of bulk potassium.

First we discuss the results for small clusters K_2 , K_4 , and K_6 (Table 1) as for these systems we can assess the accuracy of

TABLE 2: Binding Energy Per Atom (in eV) and Average Interatomic Distance $\langle R \rangle$ (in angstrom) of Potassium Clusters Containing 8 to 20 Atoms

$K_{n,m}$	$-BE/n$	$\langle R \rangle$
$K_{8,0}$	0.458	4.44
$K_{8,1}$	0.448	4.44
$K_{10,0}$	0.457	4.50
$K_{10,1}$	0.454	4.48
$K_{10,2}$	0.453	4.54
$K_{10,3}$	0.413	4.50
$K_{12,0}$	0.476	4.54
$K_{12,1}$	0.473	4.50
$K_{12,2}$	0.471	4.51
$K_{14,0}$	0.493	4.57
$K_{14,1}$	0.487	4.50
$K_{14,2}$	0.486	4.48
$K_{16,0}$	0.500	4.57
$K_{16,1}$	0.499	4.57
$K_{16,2}$	0.498	4.53
$K_{18,0}$	0.522	4.52
$K_{18,1}$	0.518	4.60
$K_{18,2}$	0.515	4.62
$K_{20,0}$	0.533	4.53
$K_{20,1}$	0.532	4.57
$K_{20,2}$	0.530	4.59
$K_{20,3}$	0.529	4.52
$K_{20,4}$	0.514	4.56

our DFT-based results by comparing them with the published data that already exist in the literature for these three clusters. In refs 29, 30, 32, and 33 the calculations on the above-

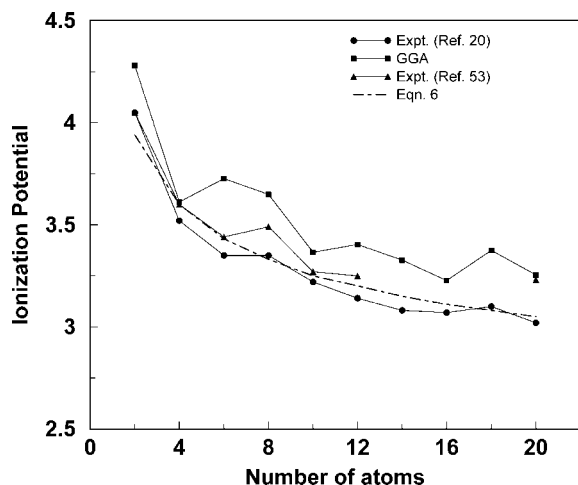


Figure 3. Plot of ionization potential (in eV) of potassium clusters containing an even number of atoms ranging from 2 to 20 atoms as a function of number of atoms. The results obtained with BP86 XC potential (solid squares) are compared with the experimental results (solid circles) and (solid triangles) results from refs 20 and 53, respectively. The continuous dotted line shows the results obtained via eq 6.

TABLE 3: Comparison of the Theoretical and Experimental IP (in eV) for K_2 , K_4 , and K_6 Clusters

ref	K_2	K_4	K_6
present (BP86)	4.28	3.61	3.73
ref 29	3.79	3.23	
ref 30	4.12	3.64	3.79
ref 32	4.32	3.43	
ref 20 (exptl)	4.05	3.52	3.35
ref 53 (exptl)	4.05 ± 0.05	3.6 ± 0.1	3.44 ± 0.1
ref 51 (exptl)	4.05 ± 0.05	3.6 ± 0.1	
ref 52 (exptl)		3.36	3.25

mentioned clusters were carried out by employing the pseudo-potential method in conjunction with the configuration interaction (CI) approach,^{29,30} the self-interaction corrected DFT³² method, and the CCSD(T) for the valence electrons.³³ On the other hand, an all-electron calculation using the techniques of Hartree–Fock theory followed by the many-body perturbation theory (MBPT) was carried out to determine the equilibrium geometries of potassium clusters up to K_7 .³¹ A DFT study with a hybrid XC potential has been carried out by Jiemchoorj et al.³⁴ It can be seen from Table 1 that for dimer, results for both BE and average interatomic distance obtained by us employing DFT are quite close to the other published data including the experimental result.⁵⁰ In fact in our result for K_2 , the BE per atom matches exactly with the experimental data and our result for interatomic distance is closest to the experimental value compared to the other theoretical data.

Following previous studies,^{29,30,32,34} we consider rhomboidal geometry for tetramer K_4 . The average interatomic distance for the tetramer geometry obtained by us is quite close to other results and the same is true for the BE per atom except for the result of ref 29. For K_6 , two geometries, namely a planar and a three-dimensional structure, have been considered for the geometry optimization. We find that the planar isomer is higher in energy than the three-dimensional one in conformity with the results of refs 30, 31, and 34. For the minimum energy structure of K_6 the difference between the results for BE and average interatomic distance obtained by us and those of refs 30, 31, and 34 is less than 10%. For K_8 we consider two structures one possessing D_{2d} symmetry¹² and another having

T_d symmetry.¹¹ We find that the D_{2d} symmetry isomer of K_8 is lower in energy than the T_d structure by around 0.08 eV. This is in contrast to the finding of ref 34, where the authors determined that the T_d structure has lower energy. It is noteworthy that Kronik et al.¹² found the same D_{2d} symmetry for Na_8 as we obtain for the lower energy structure for K_8 .

For clusters beyond Na_8 , many (more than two) isomers exist. We use all these isomers for the geometry optimization of potassium clusters. To perform the geometry optimization calculations for the clusters beyond K_8 , we sample four isomers for K_{10} , three isomers each for K_{12} , K_{14} , K_{16} , and K_{18} , and five isomers for K_{20} . These optimized structures in increasing energy order are shown in Figure 2 and their BE and average interatomic distances are presented in Table 2. We note here that for K_{20} , out of the five isomers, the higher symmetry T_d isomer does not yield minimum energy and it is for a lower symmetry D_{2d} isomer of 20 atom cluster we get the minimum energy. The energy of the T_d isomer is around 0.37 eV higher than that of the minimum energy D_{2d} structure. It is interesting to note that for the two magic number clusters K_8 and K_{20} , the minimum energy geometries possess D_{2d} symmetry, not T_d as has been reported in some studies in the literature.^{11,34} Overall, we note that our geometric results and the data from the literature agree reasonably well with each other.

Next we focus our attention on the evolution of ionization potential (IP) with the size of clusters, as this dependence has been measured extensively and these results are available in the literature.^{20,51–53} Apart from these experimental results some papers also reported theoretical results for IP of small potassium clusters at the ab initio level^{30,32} and also within SBJM.²³ To calculate IP, we restrict ourselves to only the minimum energy isomers for each cluster and employ the following formula of IP of a cluster containing n atoms:

$$IP = E(K_n^+) - E(K_n) \quad (5)$$

where $E(K_n^+)$ and $E(K_n)$ are energies of the singly charged and neutral clusters, respectively. The results of these calculations along with the data available in the literature are presented in Table 3 and Figure 3. In Table 3, we present the results for small sized potassium clusters containing 2, 4, and 6 atoms for which both theoretical and experimental results are available. For clusters containing more than 6 atoms theoretical results at the ab initio level are not available, so we compare our results with the experimental data only from refs 20 and 51–53 and these are displayed in Figure 3. From Table 3, it can be seen that for K_2 , K_4 , and K_6 , our DFT-based results for IP are quite close to other theoretical as well as experimental data. From Figure 3 it can be clearly seen that our results follow a trend that is similar to that of experimental data. However, the theoretical results are slightly overestimated with respect to the experimental ones. This may be attributed to the fact that the experiments have been performed at finite temperatures.²⁷ Here we wish to point out that Figure 3 also clearly elucidates that IP of potassium clusters decreases with increasing cluster size, which is in conformity with the conducting sphere model (CSM) of metal cluster.^{54–56} To verify this we calculate IP in accordance with the expression

$$IP = W + \frac{3}{8} \frac{e^2}{R} \quad (6)$$

where W is the bulk work function and R is the radius of the metallic droplet. Following ref 57, we use $W = 2.28$ eV and $R = r_s n^{1/3}$ (where r_s is the Wigner–Seitz radius) with $r_s = 4.86$

TABLE 4: Comparison of the Average Static Polarizability $\bar{\alpha}$ (in au) for K_2 and K_4 Clusters

method (ref)	K_2	K_4
SAOP (present)	471.2	994.1
B3PW91 (ref 34)	497.5	1013
MP2 (present)	483.2	977.8
CCSD(T) (present)	510.2	991.0
CCSD(T) (ref 33)	486.4	
CCSD(T) (ref 61)	502.1	
exptl (refs 1, 20)	486.5	
exptl (ref 62)	500 \pm 40	

TABLE 5: Average Static Polarizability $\bar{\alpha}$ and Anisotropy in Polarizability, $\Delta\alpha$, of Various Isomers of Potassium Clusters up to K_{10} in Atomic Units^a

K_n	MP2		SAOP		LDA	
	$\bar{\alpha}$	$\Delta\alpha$	$\bar{\alpha}$	$\Delta\alpha$	$\bar{\alpha}$	$\Delta\alpha$
K_2	483.2	369.1	471.02 (497.5)	336.9	437.4	289.7
K_4	977.8	931.05	994.07 (1013)	937.54	907.29	876.54
$K_{6,0}$	1308.3	754.09	1321.80 (1359)	783.22	1203.10	722.45
$K_{6,1}$	1413.8	977.49	1440.0	1011.9	1330.0	947.11
$K_{8,0}$	1492.2	301.0	1531.2	320.24	1367.5	267.88
$K_{8,1}$	1626.9	20.6	1649 (1710)	21.85	1489.4	17.45
$K_{10,0}$	2006.7	1204.3	2052.6 (1983)	1178.9	1849.4	1125.7
$K_{10,1}$	2013.4	1287.2	2052.8	1288.1	1849.8	1221.1
$K_{10,2}$	2054.0		2085.6	1161.0	1878.6	1115.1
$K_{10,3}$	2558.4	68.5	2420.5	90.70	2238.8	97.73

^aThe B3PW91 results in parentheses are taken from ref 34 for the polarizabilities of clusters from K_2 to K_{10} . These numbers are placed below the isomers having identical symmetry.

au. These results are shown in Figure 3 by a dashed line and our DFT result follows a similar trend.

B. Polarizability of Potassium Clusters. In this section we present and discuss the results of our calculations for the static dipole polarizabilities of potassium clusters. The static polarizability plays an important role in the characterization of the clusters and it is one of the properties which has been extensively measured for metal clusters specially sodium clusters.^{1,58–60} To the best of our knowledge the experimental results for static polarizabilities of some potassium clusters are available only in ref 1. Here we will compare results of our calculations for $\bar{\alpha}$ of clusters containing 2, 8, and 20 atoms with the above-mentioned experimental results.

We begin our discussion on the results for polarizabilities by first testing the accuracies of SAOP and MP2 results for dimer and tetramer against the corresponding data obtained with a large basis set coupled cluster theory with single and double excitations and perturbative triple excitation (CCSD(T)) calculations.³⁶ In Table 4 we present the results for polarizabilities of K_2 and K_4 obtained with three different methods along with the other theoretical^{33,61} and experimental^{20,62} results for the dimer which are already available in the literature. From Table 4, we notice that the results for the dimer obtained by the CCSD(T) approach vary from 486 to 510 au and these results are well within the experimental errors. The variation in the different CCSD(T) results is attributed to the use of different basis sets and also to the level of calculations (all-electron or pseudopotential). The basis set used in the present paper is

similar to the one employed in ref 61 and both are all-electron calculations and consequently two results are close to each other. The difference in the two results may be due to the use of a slightly different bond length (3.91Å) of the dimer and also inclusion of the relativistic effect in the calculation of ref 61. Furthermore, we observe that the MP2 value for the polarizability of K_2 is quite close to the lowest CCSD(T) result of ref 33, however, SAOP underestimates the polarizability by around 6% with respect to CCSD(T) results. The DFT-B3PW91 result for the polarizability of K_2 (ref 34) is also higher by around 5% than the corresponding SAOP value. This difference in the SAOP and B3PW91 results is attributed to use of the different basis sets and XC potentials in the two calculations. In contrast to the dimer case SAOP polarizability for K_4 is quite close to the CCSD(T) result and slightly higher (around 2%) than the MP2 result. Similarly, in contrast to the dimer case the difference between SAOP and B3PW91 results for K_4 is significantly reduced.

We now proceed with the calculations of static polarizabilities for all the optimized isomers shown in Figures 1 and 2. We note here that the geometries considered in this paper are nonspherical and consequently the polarizability tensors are expected to be anisotropic. We also calculate the anisotropy in polarizability given by

$$|\Delta\alpha| = \left[\frac{3\text{Tr}\alpha^2 - (\text{Tr}\alpha)^2}{2} \right]^{1/2} \quad (\text{general axes}) \quad (7)$$

where α is the second-rank polarizability tensor.

The two methods (MP2, and TDDFT) which we employ to calculate the static polarizabilities of clusters take into account the electron correlations in different ways and thereby enable us to check the consistencies of our results, as no systematic theoretical results are available in the literature for comparison (except one study³⁴ restricted up to $n = 10$). In Tables 5 (K_2 – K_{10}) and 6 (K_{12} – K_{20}) we present results for the average static polarizability $\bar{\alpha}$ and anisotropy in the polarizability $\Delta\alpha$ obtained with MP2 and TDDFT (with SAOP and LDA XC potentials) methods. For the sake of comparison we also present the results of ref 34 (in parentheses) in Table 5. We have performed MP2 calculations of $\bar{\alpha}$ and $\Delta\alpha$ for clusters only up to K_{14} and K_{10} , respectively. We note from Tables 5 and 6 that the results for both polarizabilities and their anisotropies obtained by MP2 and TDDFT-SAOP are quite close for all the clusters while the corresponding LDA values are systematically underestimated. SAOP results for all the isomers for each cluster are actually slightly higher than the corresponding MP2 data except for K_2 . We also observe from Table 5 that the DFT-B3PW91 values of polarizability for all the clusters (except K_{10}) are slightly higher than both SAOP and MP2 results. As pointed out earlier these differences may be due to the use of different basis sets, XC potentials, and values of bond length in the two calculations. To study the evolution of polarizability $\bar{\alpha}$ and anisotropy in polarizability $\Delta\alpha$ with the size, we plot them in Figure 4, panels a and b, respectively, for the minimum energy isomers of each cluster as a function of the number of atoms. In this figure we also display experimental data for three magic clusters, namely, K_2 , K_8 , and K_{20} .¹ Figure 4 once again clearly shows that MP2 results for the polarizabilities and anisotropies in polarizabilities are very close to the corresponding SAOP results and LDA values are systematically lower than both of them. Both SAOP and MP2 results for the polarizabilities for magic number clusters K_2 , K_8 , and K_{20} are well within the experimental error bars (of the order of ± 5 –7%). The maximum difference between the experimental and SAOP as well as MP2

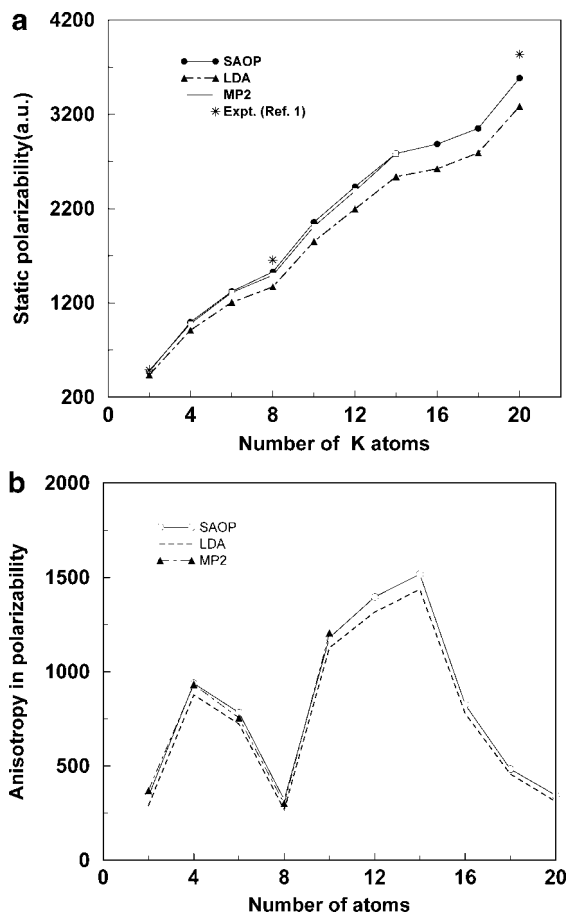


Figure 4. Plot of (a) average static polarizability $\bar{\alpha}$ (in au) and (b) anisotropy in polarizability $\Delta\alpha$ (in au) for minimum energy isomers of potassium clusters as a function of number of particles. The experimental results for the polarizabilities of magic clusters K_2 , K_8 , and K_{20} ¹ are also shown in this figure. The lines joining the points are a guide to the eye.

TABLE 6: Same as Table 5 but for K_{12} to K_{20}

K_n	MP2		SAOP		LDA	
	$\bar{\alpha}$	$\Delta\alpha$	$\bar{\alpha}$	$\Delta\alpha$	$\bar{\alpha}$	$\Delta\alpha$
$K_{12,0}$	2385.4		2429.4	1395.4	2194.6	1315.7
$K_{12,1}$	2448.2		2483.1	1461.8	2259.6	1390.5
$K_{12,2}$	2380.7		2417.9	1467.8	2186.2	1373.6
$K_{14,0}$	2781.6		2782.3	1516.3	2536.4	1434.6
$K_{14,1}$	2766.6		2762.3	1536.9	2517.9	1448.9
$K_{14,2}$	2661.6		2733.9	1255.6	2472.8	1205.9
$K_{16,0}$			2883.2	825.4	2619.6	778.6
$K_{16,1}$			2878.9	816.9	2614.5	769.4
$K_{16,2}$			2990.9	912.4	2722.3	878.4
$K_{18,0}$			3048.7	483.1	2787.7	456.0
$K_{18,1}$			3216.3	623.7	2912.5	568.0
$K_{18,2}$			3197.7	801.9	2894.0	744.4
$K_{20,0}$			3582.2	344.40	3220.4	184.4
$K_{20,1}$			3604.3	140.1	3289.1	120.8
$K_{20,2}$			3526.4	539.3	3203.0	475.2
$K_{20,3}$			3518.6	204.4	3220.4	184.8
$K_{20,4}$			4066.1	6.35	3769.8	6.58

results is observed for the K_{20} cluster. Note also (from Tables 5 and 6) that both SAOP and MP2 results for the polarizabilities of clusters K_8 and K_{20} possessing T_d symmetry ($K_{8,1}$ and $K_{20,4}$) are closer to the corresponding experimental data (K_8 , $\bar{\alpha}_{\text{exp}} =$

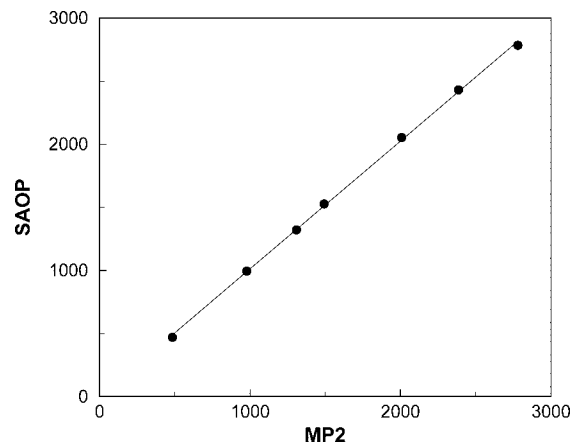


Figure 5. Plot of SAOP results for average static polarizability $\bar{\alpha}$ against corresponding MP2 values. All the results are in atomic units and the straight line is a least-squares fitted line.

1653 ± 83 au and for K_{20} $\bar{\alpha}_{\text{exp}} = 3834 \pm 300$ au)²⁰ than their respective minimum energy structures (see Tables 5 and 6). From these results it may be inferred that for these two clusters the geometries detected in the experiments performed at finite temperatures may be different from what have been obtained as lowest energy structures in this paper by zero-temperature DFT-based calculations. Overall, we conclude from the results of Tables 5 and 6 and Figure 4 that TDDFT-based calculations with SAOP yield results for polarizability that are reasonably accurate and compare well with the correlated wave function based MP2 results as well as experimental data, where available.

It has already been pointed out that MP2 calculations are computationally expensive and thus it becomes increasingly difficult to apply this method for very large clusters (more than 10 atoms). However, a good match between SAOP and MP2 results for clusters up to K_{14} encourages us to explore how the two results scale with respect to each other. To this end we plot SAOP and MP2 results along y - and x -axes, respectively, in Figure 5 and fit the data points with a straight line by least-squares fitting. It can be clearly seen from Figure 5 that a very good fitting is obtained with the correlation coefficient value 0.9997 signifying a linear relationship between SAOP and MP2 results. This linear relationship between SAOP and MP2 will enable us to predict MP2 results for the polarizability of larger clusters.

According to the jellium model, clusters with closed shells of delocalized electrons have spherical shape.^{2,3} It is well-known that polarizability of such a sphere is proportional to the volume of the sphere. Since the geometries of clusters considered in this paper are, in general, not spherical in nature, thus such linear dependence of polarizability with the volume of cluster is not very obvious. However, the studies on the relationship between the static polarizability and the volume of carbon and sodium clusters have already been reported in the literature.^{13,17,63} Here we extend this study for potassium clusters and we go up to clusters containing 20 atoms. For this purpose we use SAOP results for the polarizabilities of lowest energy isomers for each cluster and obtain its volume by using the prescription of Tomasi and Persico.⁶⁴ The plot of the polarizability as a function of the volume of the clusters is shown in Figure 6. It can be clearly seen from this figure that a good fitting is obtained with the correlation coefficient value of 0.996. This result then clearly suggests that a good correlation exists between the polarizability and the cluster volume even for nonspherical potassium clusters. This linear correlation between the polarizability and volume

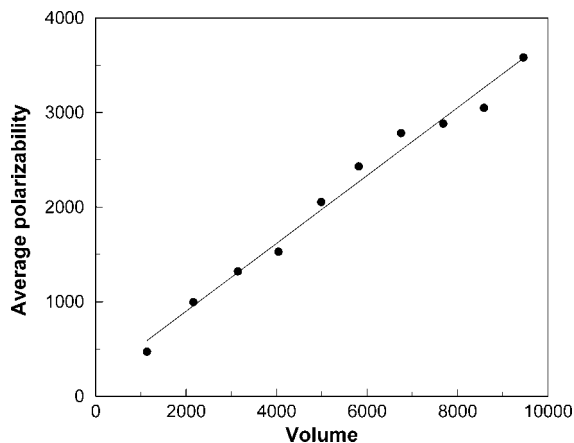


Figure 6. Plot of average static polarizability $\bar{\alpha}$ obtained with SAOP as a function of the cluster volume. All the results are in atomic units and the straight line is a least-squares fitted line.

is an important result as it enables us to construct a size-to-property relationship for polarizability. Using this relationship polarizabilities of larger clusters can be calculated as for these clusters performing ab initio calculations are computationally expensive if not impossible.

We wish to close this paper with a comparison of the SJBM results with the ab initio results presented in this paper. The jellium-based results within DFT for the polarizability of K_8 , and K_{20} are available in the literature²¹ and we compare them with corresponding ab initio TDDFT results. The LDA calculations in ref 21 were performed by employing the Dirac form for the exchange and the Wigner form for the correlation energy functionals.⁶⁵ On the other hand, in this paper we employ VWN parametrization of the LDA XC functional, which uses the same Dirac exchange energy functional, but the parametrization for the correlation part is different from that of the Wigner functional. We expect that the deviation in the results due to application of different correlation energy functionals will be significantly smaller than the difference in the two results, arising due to the consideration of structures of the clusters in ab initio calculations. The results for the polarizabilities of K_8 and K_{20} clusters calculated with the LDA XC functional in the jellium model are found to be $\alpha_{K_8} = 1212$ au and $\alpha_{K_{20}} = 2939$ au. In comparison to this our ab initio results (for the minimum energy geometries) with the LDA XC potential are $\alpha_{K_8} = 1367$ au and $\alpha_{K_{20}} = 3220$ au. Besides LDA, Rubio et al.²¹ also employed a potential with correct $-1/r$ asymptotic decay as introduced by Przybylski and Borstel (PB)⁶⁶ within the weighed density approximation (WDA) to calculate the polarizability. We compare the results obtained with PB potential within the jellium model ($\alpha_{K_8} = 1542$ au and $\alpha_{K_{20}} = 3489$ au) with SAOP results ($\alpha_{K_8} = 1531$ au and $\alpha_{K_{20}} = 3582$ au) as SAOP too possesses correct asymptotic behavior. The jellium-based LDA results are around 10% lower than the corresponding TDDFT-based ab initio values. On the other hand, differences between ab initio SAOP and PB within the jellium model results are even smaller. We note here that a similar observation for the polarizabilities of sodium clusters was made in ref 11. From the closeness of the results obtained by employing ab initio and SJBM, we conclude that for the alkali-metal atom clusters detailed ionic core structures may not have much influence on the values of the cluster polarizabilities.

IV. Conclusion

This paper is devoted to ab initio calculations of various properties of different possible isomers of potassium clusters

containing an even number of atoms ranging from 2 to 20. To perform the calculations we choose different configurations possessing symmetry elements similar to those of sodium clusters available in the literature. These geometries are then optimized by employing the DFT-based method with the TZ2P basis set and the GGA XC potential. For small clusters up to 10 atoms the results of our calculations for BE per atom, bond length, and average interatomic distance match quite well with the other published data wherever available. We have also studied from these DFT-based calculations evolution of IP with the size of clusters. The experimental data for the size dependence of IP of potassium clusters is available in the literature and our ab initio DFT-based results match quite well with them.

In this paper we have carried out calculations of the static polarizabilities of the potassium clusters with MP2 and TDDFT approaches as well as CCSD(T) (for dimer and tetramer) taking electron correlations in different ways. A model XC potential (SAOP) possessing correct behaviors both in the asymptotic and inner regions of the molecule and also less accurate LDA XC potential have been used to calculate polarizabilities within TDDFT. For all the calculations sufficiently large basis sets have been employed. For dimer and tetramer the results for the polarizabilities obtained by different methods, employed in this paper, agree with each other. Similarly for clusters beyond K_4 and up to K_{14} MP2 and SAOP results for the polarizabilities are quite close to each other. We find a very good linear correlation between MP2 and SAOP results. On the other hand, TDDFT-based calculations with LDA XC potentials are systematically lower than those of MP2 and SAOP. Moreover, we also find that both SAOP and MP2 results for the static polarizabilities of 2-, 8-, and 20-atom potassium clusters agree quite well with the experimental results. In general it is observed that for both sodium and potassium clusters the SAOP data for the polarizability are higher than the corresponding MP2 results. In this paper we have also investigated the volume-to-polarizability scaling for the potassium clusters. Our study has found a very good linear correlation between the volume and polarizability of the clusters. This scaling law can be exploited to determine the polarizabilities of larger clusters. Finally we have also compared the SJBM-based results for the polarizabilities of K_8 and K_{20} with our corresponding ab initio values obtained by employing TDDFT. This comparison clearly reveals that the jellium model based results for the polarizabilities are quite accurate for magic number clusters and it is expected that this model is increasingly more suitable for such larger clusters.

Acknowledgment. A.B. and A.C. wish to thank Pranabesh Thander of RRCAT Computer Centre for his help and support in providing uninterrupted computational resources and also for smooth running of the codes and C. Kamal for his help in geometry optimization. It is a pleasure to thank Prof. Vitaly Kresin for his valuable suggestions and making some experimental data available to us.

References and Notes

- (1) Knight, W. D.; Clemenger, K.; de Heer, W. A.; Saunders, W. A. *Phys. Rev. B* **1985**, *31*, 2539.
- (2) (a) Brack, M. *Rev. Mod. Phys.* **1993**, *65*, 677, and references cited therein. (b) de Heer, W. A. *Rev. Mod. Phys.* **1993**, *65*, 611.
- (3) Alonso J.; Balbas, L. C. *Topics in Current Chemistry*; Springer-Verlag: Berlin, Germany, 1996; Vol. 182 and references cited therein.
- (4) Madjet, M.; Guet, C.; Johnson, W. R. *Phys. Rev. A* **1995**, *51*, 1327.
- (5) Moullet, I.; Martins, J. L.; Reuse, F.; Buttet, J. *Phys. Rev. B* **1990**, *42*, 11598.
- (6) Rothlisberger, U.; Andreoni, W. *J. Chem. Phys.* **1991**, *94*, 8129.

- (7) Guan, J.; Casida, M. E.; Köster, A. M.; Salahub, D. R. *Phys. Rev. B* **1995**, *52*, 2184.
- (8) Calmanici, P.; Jug, K.; Köster, A. M. *J. Chem. Phys.* **1999**, *111*, 4613.
- (9) Kümmel, S.; Berkus, T.; Reinhard, P.-G.; Brack, M. *Eur Phys. J. D* **1999**, *11*, 239.
- (10) van Gisbergen, S. J. A.; Pacheco, J. M.; Baerends, E. J. *Phys. Rev. A* **2001**, *63*, 063201.
- (11) Solovyov, I. A.; Solovyov, A. V.; Greiner, W. *Phys. Rev. A* **2002**, *65*, 053205.
- (12) Kronik, L.; Vasiliev, I.; Chelikowsky, J. R. *Phys. Rev. B* **2000**, *62*, 9992.
- (13) (a) Chandrakumar, K. R. S.; Ghanty, T. K.; Ghosh, S. K. *J. Chem. Phys.* **2004**, *120*, 6487. (b) Chandrakumar, K. R. S.; Ghanty, T. K.; Ghosh, S. K. *J. Phys. Chem. A* **2004**, *108*, 6661.
- (14) Maroulis, G. *J. Chem. Phys.* **2004**, *131*, 10519.
- (15) Jiemchoorj, A.; Norman, P.; Sernelius, B. E. *J. Chem. Phys.* **2006**, *125*, 124306.
- (16) Sophy, K. B.; Calaminici, P.; Pal, S. *J. Chem. Theory Comput.* **2007**, *3*, 716.
- (17) Banerjee, A.; Chakrabarti, A.; Ghanty, T. K. *J. Chem. Phys.* **2007**, *127*, 134103.
- (18) Chandrakumar, K. R. S.; Ghanty, T. K.; Ghosh, S. K. *Int. J. Quantum Chem.* **2005**, *105*, 166.
- (19) (a) Boustani, I.; Pewestorf, W.; Fantucci, P.; Bonačić-Koutecky, V.; Koutecky, J. *Phys. Rev. B* **1987**, *35*, 9437. (b) Bonačić-Koutecky, V.; Fantucci, P.; Koutecky, J. *Phys. Rev. B* **1988**, *37*, 4369.
- (20) (a) Saunders, W. A.; Clemenger, K.; de Heer, W. A.; Knight, W. D. *Phys. Rev. B* **1985**, *32*, 1366. (b) Saunders, W. A. Ph.D. Thesis, 1986.
- (21) Rubio, A.; Balbas, L. C.; Serra, L.; Barranco, M. *Phys. Rev. B* **1990**, *42*, 10950.
- (22) (a) Kresin, V. *Phys. Rev. B* **1989**, *39*, 3042. (b) Kresin, V. *Phys. Rev. B* **1990**, *42*, 3247.
- (23) Balbas, L. C.; Alonso, J. A.; Rubio, A. *Eur. Phys. Lett.* **1991**, *14*, 323.
- (24) Yannouleas, C.; Vigezzi, E.; Broglia, R. *Phys. Rev. B* **1993**, *47*, 9849.
- (25) Pacheco, J. M.; Ekardt, W. *Mod. Phys. Lett. B* **1993**, *7*, 573.
- (26) Alasia, F.; Serra, L.; Broglia, R.; Van Giai, N.; Lipparini, E.; Roman, H. E. *Phys. Rev. B* **1995**, *52*, 8488.
- (27) Yannouleas, C.; Landmann, U. *Phys. Rev. Lett.* **1997**, *78*, 1424.
- (28) Pohl, A.; Reinhard, P.-G.; Sarud, E. *Phys. Rev. A* **2003**, *68*, 053202.
- (29) Pacchioni, G.; Beckmann, H.; Koutecky, J. *Chem. Phys. Lett.* **1982**, *87*, 151.
- (30) Spiegelmann, F.; Pavolimi, D. *J. Chem. Phys.* **1988**, *89*, 4954.
- (31) Ray, A. K.; Altekar, S. D. *Phys. Rev. B* **1990**, *42*, 1444.
- (32) Flad, J.; Igel, G.; Dolg, M.; Stoll, H.; Preuss, H. *Chem. Phys.* **1983**, *75*, 331.
- (33) Lim, I. S.; Schwerdtfeger, P.; Sohnel, T.; Stoll, H. *J. Chem. Phys.* **2005**, *122*, 134307.
- (34) Jiemchoorj, A.; Sernelius, B. E.; Norman, P. *J. Comput. Methods Sci. Eng.* **2007**, *7*, 475.
- (35) Frisch, M. J.; Head-Gordon, M.; Pople, J. A. *Chem. Phys. Lett.* **1990**, *166*, 275.
- (36) Piecuch, P.; Kucharski, S.; Kowalski, K.; Musial, M. *Comput. Phys. Commun.* **2002**, *149*, 71.
- (37) Lai, S. K.; Hsu, P. J.; Wu, K. L.; Liu, W. K.; Iwamatsu, M. *J. Chem. Phys.* **2002**, *117*, 10715.
- (38) (a) Becke, A. D. *Phys. Rev. A* **38** **1988**, 3098. (b) Perdew, J. P. *Phys. Rev. B* **1986**, *33*, 8822.
- (39) (a) Jensen, L.; Zhao, L.; Schatz, G. C. *J. Phys. Chem. C* **2007**, *111*, 4756. (b) Guerra, C. F.; Bickelhaupt, F. M.; Snijders, J. G.; Baerends, E. J. *J. Am. Chem. Soc.* **2001**, *122*, 4117. (c) van Gisbergen, S. J. A.; Rosa, A.; Ricciardi, G.; Baerends, E. J. *J. Chem. Phys.* **1999**, *111*, 2499.
- (40) van Gisbergen, S. J. A.; Snijders, J. G.; Baerends, E. J. *J. Chem. Phys.* **1998**, *109*, 10657.
- (41) Banerjee, A.; Harbola, M. K. *Phys. Rev. A* **1999**, *60*, 3599.
- (42) Gritsenko, O. V.; Schipper, P. R. T.; Baerends, E. J. *Chem. Phys. Lett.* **1999**, *302*, 199.
- (43) Schipper, P. R. T.; Gritsenko, O. V.; van Gisbergen, S. J. A.; Baerends, E. J. *J. Chem. Phys.* **2000**, *112*, 1344.
- (44) Baerends, E. J.; Autscbach, J.; Berces, A. et al. *Amsterdam Density Functional; Theoretical Chemistry; Virje Universiteit: Amsterdam, The Netherlands*, URL <http://www.scm.com>.
- (45) Schmidt, M. W.; BalDridge, K. K.; Boatz, J. A.; Elbert, S. T.; Gordon, M. S.; Jensen, J. H.; Koseki, S.; Matsunaga, N.; Nguyen, K. A.; Su, S. J.; Windus, T. L.; Dupuis, M., Jr. *Comput. Chem.* **1993**, *14*, 1347.
- (46) Sadlej, A. J.; Urban, M. *J. Mol. Struct. (THEOCHEM)* **1991**, *234*, 147.
- (47) van Gisbergen, S. J. A.; Snijders, J. G.; Baerends, E. J. *J. Chem. Phys.* **1995**, *103*, 9347.
- (48) Gross, E. K. U.; Dobson, J. F.; Petersilka, M. *Top. Curr. Chem.* **1996**, *181*, 81.
- (49) Vosko, S. H.; Wilk, L.; Nussair, M. *Can. J. Phys.* **1980**, *58*, 1200.
- (50) Huber, K. P.; Herzberg, G. *Constants of Diatomic Molecules*; Van Nostrand: Princeton, NJ, 1977.
- (51) Hermann, A.; Schumacher, E.; Woste, L. *J. Chem. Phys.* **1978**, *68*, 2327.
- (52) Brechignac, C.; Cahuzac, Ph.; Roux, J. Ph. *J. Chem. Phys.* **1986**, *127*, 445.
- (53) Kappes, M. M.; Schar, M.; Radi, P.; Schumacher, E. *J. Chem. Phys.* **1986**, *84*, 1863.
- (54) Cini, M. *J. Catalysis* **1975**, *37*, 187.
- (55) Wood, D. M. *Phys. Rev. Lett.* **1981**, *46*, 749.
- (56) Perdew, J. P. *Phys. Rev. B* **1988**, *37*, 6175.
- (57) Brechignac, C. *Clusters of Atoms and Molecules: Theory, Experiment, and Clusters of Atoms*; Haberland, H., Ed.; Springer-Verlag: Hiedelberg, Germany, 1994.
- (58) Brechignac, C.; Cahuzac, Ph.; Leygnier, J.; Weiner, J. *J. Chem. Phys.* **1989**, *90*, 1492.
- (59) Rayane, D.; Allouche, A. R.; Benichou, E.; et al. *Eur. Phys. J. D* **1999**, *9*, 243.
- (60) Tikhonov, G.; Kasperovich, V.; Wong, K.; Kresin, V. *Phys. Rev. A* **2001**, *64*, 063202.
- (61) Urban, M.; Sadlej, A. J. *J. Chem. Phys.* **1995**, *103*, 9692.
- (62) Tarnovsky, V.; Bunimovicz, M.; Vuskovi, L.; Stumpf, B.; Bederson, B. *J. Chem. Phys.* **1993**, *98*, 3894.
- (63) Ghanty, T. K.; Ghosh, S. K. *J. Phys. Chem.* **1993**, *97*, 4951.
- (64) Tomasi, J.; Persico, M. *Chem. Rev.* **1994**, *94*, 2027.
- (65) *The Inhomogenous Electron Gas*; March, N. H., Lundqvist, B. I., Eds.; Plenum: New York, 1983.
- (66) Przybylski, H.; Borstel, G. *Solid State Commun.* **1984**, *49*, 317.